Analysis on the Weather Circumstance Involved in the UH-60M Helicopter Incident on 2 January 2020

Tai-Hwa Hor[1], Tian-Yow Shyu[2], Hung-Yang Tseng[3]
General Education Center, Lunghwa University of Science and Technology[1]
Center for General Education, Taipei City University of Science and Technology[2]
Department of Atmospheric Sciences, Chinese Culture University[3]

Abstract

At 0807 TST (UTC+8) on 2 January 2020, an UH-60M Black Hawk helicopter of the Republic of China Air Force (ROCAF) in Taiwan crashed at a mountainside over the north island, killing 8 people on board, including three high-ranked generals in the Ministry of National Defense. The study tries to focus on the mesoscale analysis of weather conditions (wind speed, wind direction, visibility, relative humidity, local circulation, turbulence, etc.) embedded within the weak NE monsoon under the 850 hPa level, especially mentioning the cloud/fog initiation in the complex terrains of Snow Mountain Range, the northernmost range in Taiwan running from northeast to southwest.

Based upon the mesonet surface data analysis, we learned that the local convergence of prevailing easterly wind and land breeze over the northeast corner of Taiwan was the primary weather circumstance in the early morning, bringing abundant moisture inland, triggering the cloud/fog generation and maintaining its development. Also, the vertical cross section along 24.5°N between 120.1°E and 122.5°E delivered more reliable evidences, mentioning a locally vertical circulation with obvious upward motions in magnitude of 10^{-2} m/s under the 850 hPa level over the plain area and slight downward motions over the complex terrains. Visibility forecast illuminated the worst visibility was in the range of the 0-50 m over the complex terrains. It preliminarily concludes that the persistent low cloud/fog and the unstable flow over the complex terrain might reduce the reliability of visibility and increased the flight risk in VFR (visual flight rules). Those weather conditions will threat the aviation safety greatly.

Keywords: satellite analysis, mesonet surface data analysis, WINS, helicopter accident.

1. Introduction

Helicopter is one type of aircrafts with one or more power-driven horizontal propellers or rotors that enable it to take off and land vertically, to move in any direction, or to remain stationary in the air. Also, due to its handling properties under low airspeed conditions, it has been chosen to conduct tasks that were previously not possible with other aircrafts. Today, helicopter uses include transportation of people and cargo, military uses, construction, firefighting, search and rescue, tourism, medical transport, law enforcement, agriculture, news and media, and aerial observation, and so on. However, the accident rate of helicopter worldwide remains at a high level because helicopters are typically used in dangerous situations where airplanes are unable to fly such as flying low near obstacles like buildings, TV/radio towers, electrical wires, wind turbine and topography. All of these situations put helicopters, their passengers and people on the ground at risk.

According to the statistics, the safety of western-built civil turbine helicopters in 2018, as measured globally by the fatal accident rate, was more or less within the long-term trend but, as noted in previous years, this improvement is still only just keeping up with the growth of the industry. While accident rates, on average, have been getting better over the last 20 or so years, the frequency of accidents - the number of fatal accidents and fatalities suffered by this class of aircraft each year - is only reducing slowly (Hayes, 2019). Shown in Table 1, the 2018 numbers were slightly worse than in 2017, but still more or less in line with expectations. Based on the news issued by US Helicopter Safety Team (USHST, 2020), total accidents and the number of fatal accidents for the US civil helicopter industry remained flat during 2019, and the annual numbers also remained below accident totals from five and six years ago (Table 2). Preliminary data shows 122 total US helicopter accidents in 2019 compared to 121 accidents the year before. A 16% decrease in accidents in 2019 compared to the total accidents in 2013. Over the past two decades, the US helicopter fatal accident rate has been cut in half, from 1.27 fatal accidents per hundred thousand hours to 0.63 (based on a five-year rolling average). Unfortunately, according to preliminary data, the total fatal accident rate per hundred thousand hours was 0.80 for 2019 (Helicopter Safety News, 2020), which was much higher than the five-year rolling average of 0.63. It does deserve to pay a lot of attention on helicopter flight safety in the future. However, the fatal accident rate per hundred thousand hours decreased to 0.63 for January-June 2020, and this decrease results from a decrease in flights during the COVID-19 outbreak. Hogan (2014) organized a number of things for causes of helicopter crashes in US, including pilot error, defective parts, inefficient maintenance or repair, weather conditions, on-ground hazards, excessive loads, air traffic controller error, pilot inexperience.

In Taiwan, the ten-year average rate of accident with government helicopters between 2001 and 2010 was 10.08 times per hundred thousand hours, including fatal and non-fatal accidents (Tsai, 2013). In addition to military use, government helicopters are the major type of aircraft in frequent use for diverse functions. However, the major risk factors in aviation mission can contribute to flight safety, including the performance of helicopter, weather conditions, night time aviation, and environmental conditions. Also, the flight risk of UIMC (unintended flight in instrument meteorological conditions) was quite significant due to the critical factors of spatial disorientation, ability of instrument flight rules, equipment of flight navigation and auto pilot (Tsai, 2013). Especially, the combination of weather conditions and environmental conditions (complex and mountainous terrain, high-voltage electric cables and towers, transport cage wires, etc.) are the primary factors for the risk increase.

Usually, the criterion of VFR (visual flight rules) for helicopters is 1600 m in visibility and 500 ft in cloud ceiling. Previous study (Liu, 2008) mentioned that a ROC Army UH-1H helicopter hit the 45-m high radio tower at top of Zhong-liao Mountain (mountain ridge 421 m), Chi-shan District, Kaohsiung, south of Taiwan, at 1604 TST (UTC+8) of 3 April 2008 under the intense NE monsoon situation, and killed 8 military officers and soldiers on board. Most of time in winter time, after the passage of cold front, the NE monsoon prevailed over the Taiwan area, bringing adverse weather conditions, e.g., deep cloud with low ceiling, strong wind and drizzle/thick fog. Both of poor visibility (reported to be 5 m) and turbulence phenomena over the complex terrain resulted in the fatal accident. Also, Hor, etc., (2020) delineated that the wave-like echoes organized by deep convections embedded within the rainband of Typhoon Matmo (2014) featured a key factor on the development of short duration heavy rainfall, low visibility and significant turbulence from the mesoscale point of view. Therefore, the TransAsia Airways GE222 aircraft faced multiple and severe weather situations, including the intense crosswind, obvious downdraft/updraft and extremely low visibility before it crashed in the vicinity of Makung Airport, Punghu Island, about 45-km off the southwestern coast of Taiwan, at 1906 TST (UTC+8) on 23 July 2014 when conducting the RWY 20 VOR approach, causing 48 fatalities and 10 serious injuries, 5 residents on ground suffered minor injuries. The typhoon-related rainband on aviation safety was remarkable, and it is an unforgettable case for flight risk in weather conditions.

In the early morning of 2 January 2020, a ROC Air Force Rescue Group helicopter took off from Songshan Air Base near the capital Taipei, on a flight to Dong-ao-ling Radar Station, Su-ao, Yilan County, an air force base in the northeast of Taiwan. Unfortunately, it crashed in the Wulai District of New Taipei City, Taiwan, while executing a VIP transport mission. The fatal accident of Sikorsky UH-60M helicopter killed eight, including armed forces leader Gen. Shen Yi-Ming. The helicopter lost contact with Songshan Air Base at 0807 TST (UTC+8), thirteen minutes after taking off. Reports suggested the crash occurred in rapidly changing weather conditions (e.g., cloudy/foggy conditions). However, before the crash, the crew radioed that weather conditions were acceptable (Hsiang, etc., 2020). The Black Hawk helicopter is perfect for rescue mission at altitudes above 2,000m or at sea at nighttime. Its best feature is nighttime reconnaissance. Therefore, more detailed investigation needs to step forward in order to identify the realistic scenario through the multi-scale processes based upon the synoptic scale, mesonet and remote sensing analyses.

Therefore, the goals of this study will cover:

a. Describe the characteristics of the local circulation embedded within the NE monsoon and land/sea breeze through the multi-scale processes.

b. Realize the possible causes of the Black Hawk helicopter occurrence from the perspective of weather conditions and on-ground hazards.

2. Data Resources and Methodology

2.1 Data Resources

By using the weather observation data, forecast data, radar reflectivity maps, satellite imageries adopted from the Central Weather Bureau (CWB), the National Science and Technology Center for Disaster Reduction (NCDR), and the Air Force Weather Wing of Taiwan as well as NCEP reanalysis data, this study focuses on the local circulation influenced by NE monsoon and land/sea breeze over the Yilan Plain and the complex terrains in the northeast part of Taiwan. Also, it tries to delineate the characteristics of the flow pattern, vertical velocity and relative humidity embedded within the local circulation, and the related weather conditions in the lower atmosphere.

2.2 Methodology

The primary approaches conducted in this study include the mesonet surface analysis, remote sensing analysis, conceptual model integration based on the available meteorological data.

3. Synoptic Weather Analysis

The weather pattern in winter time during the Taiwan area is deeply influenced by the Siberian high system and the related NE monsoon, bringing cold temperature, strong wind and abundant moisture accumulation due to the intense pressure gradient over ocean. The surface weather map at 0000UTC on 2 January 2020 mentioned that the southeastward movement of split high in slight pressure gradient was located at the East China Sea and it brought weak NE monsoon over the north Taiwan area. The composite mean surface vector wind distribution in synoptic scale on 2 January 2020 over the Northwest Pacific Ocean was shown in Fig. 1(a) analyzed by NOAA/ESRL (2020), and it told the strong NE monsoon was prevailing over the open ocean with weak NE wind over the Taiwan area. Also, the composite mean sea surface temperature on 2 January 2020 was mentioned in Fig. 1(b), giving an obvious temperature gradient over the Taiwan area, and giving a favorable circumstance for moisture delivery from northeast to southwest. Fig. 1(c), the composite mean relative humidity in 1000hPa level on 2 January 2020, supported the finding, an abundant moisture distribution (RH>80%) over the Taiwan area. Again, the composite mean omega distribution in 1000hPa level on 02 January 2020 illuminated the slight vertical motion in the vicinity of Taiwan, a feasible condition for local circulation and cloud formation shown in Fig. 1(d).

Furthermore, the vertically atmospheric profile shown in the skew T log P diagram at Hualian weather station, located at a seashore site of the east part of Taiwan, at 0800TST (UTC+8) on 02 January 2020 identified an evident inversion located at about the 780 hPa level with NE wind in the lower layer (below 850 hPa) and westerly wind in the upper layer (above 700 hPa) (Central Weather Bureau, 2020). Also, the air was almost saturated below the inversion layer, and it's a feasible condition for cloud triggering. Similar situation occurred in the profile at Taipei weather station except the air in the lower atmosphere became quite dry resulting from the moisture blockage by surrounding terrains and mountains .

From the synoptic point of view, the north part of Taiwan was under a weather pattern of weak NE monsoon and it's a favorable situation for the initiation of local circulation over the Yilan plain.

4. Mesoscale Weather Analysis

4.1. Local Circulation Feature

Under the large scale weather conditions of weak NE monsoon and abundant moisture supply over the north Taiwan on 2 January 2020, an obviously local convergence zone was formed over the Yilan Plain at 0700TST (UTC+8) and 0800TST (UTC+8) shown in Fig. 2 because of the interaction of weak NE wind and land breeze. However, the consecutively composite radar reflectivity maps from 0500TST to 0800TST (UTC+8) on 2 January 2020 featured the convective line echo pattern off the east coast of Taiwan were moving southward, but they couldn't identify the similar convergent situation owing to the radar echo blocking by mountainous areas over the Yilan Plain and complex terrains. About the previous studies on location and timing of the convective lines off the southeastern Taiwan from long-term radar observations learned that the low-level convergence in nearshore regions and the interaction of atmosphere and SST gradient associated with Kuroshio were the primary mechanisms for its formation (Yu, et al., 2008; Lin, et al., 2016).

The more evident findings based on the WINS (Weather Integration and Nowcasting System) data of CWB at 0200TST (UTC+8) on 2 January 2020 delivered reliable facts related with the characteristics of local circulation (shown in Fig. 3(a)). The vertical cross section of relative humidity (%), omega (- ubar/s) and wind speed (kts) along 24.5^{o}N between 120.1^{o}E and 122.5^{o}E mentioned that the local circulation and slight vertical motion in magnitude of 10^{-2} m/s with high relative humidity under the 850 hPa level over the Yilan Plain, and the weak downward motion over the complex terrains were observed, while the westerly flow was dominated above 2000m in altitude. Again, six hours later, the similar situation at 0800TST (UTC+8) on 2 January 2020 still occurred, but the intensity of local circulation and relative humidity became weaker (shown in Fig. 3(b)).

4.2. Visibility Forecast

After the integration of the primary findings of adequate moisture supply and weak NE flow in large scale as well as the generation of local convergence and circulation in meso scale could trigger the formation of cloud/fog in the lower layer. Therefore, the NCDR announced visibility forecast valid at 0500 TST (UTC+8) of 2 January 2020 based on the observation of 0200 TST of 2 January 2020. The forecast offers the visibility difference initiated by the surface fog, excluding the effect of air pollution. The low visibility area covered the most of the complex terrains in the west of Yilin Plain, with the lowest magnitude of 0~50 m. Six hours later (0800 TST), the low visibility area still covered the complex terrains with the lowest magnitude of 50~200 m.

5. Satellite Sensing Analysis

The composite reflectivity from long-term radar observations was a reliable tool to reconnaissance the initiation and development of low cloud/fog usually. However, the area over the Yilan Plain and the complex terrain was radar blind spot, and radar echoes couldn't identify the significant weather phenomena. The only reliable approach for remote sensing was satellite imageries.

Based upon the information presented by the Japan Meteorological Agency (2016), characteristics of primary wavebands of AHI (Advanced Himawari Imager) include:

a. VS (0.64µm): The waveband of the strongest solar radiation with spatial resolution of 0.5 km.

b. IR (10.4µm): The waveband of the strongest earth radiation with little intermediate absorption and re-emission (atmospheric window). The spatial resolution is 2.0 km.

c. I4 (3.9µm): Affected by both solar and earth radiation. The radiation characteristic for water cloud is different from that of IR, which enables visualization of low-level cloud (fog) at night with spatial resolution of

2.0 km.

Moreover, true color image comes from combination of data in visible bands of red (0.64μm), green (0.51μm) and blue (0.47μm) modified by Rayleigh scattering. For the purpose of data continuity, nighttime images are produced by using the GeoColor algorithm, which is composed of infrared channel (10.8μm) and near-infrared channel (3.9μm), and which uses city lights as a static background (CWB, 2020).

Comparing the radar reflectivity and the true color satellite image in Fig. 4 at 0700TST and 0800TST on 2 January 2020, the persistent low cloud/fog over the complex terrain could be identified clearly from the true color satellite images. Furthermore, the visible satellite images gave more reliable evidence for low cloud/fog with higher spatial resolution of 0.5 km.

6. Discussions and Conclusions

The Himawari IR satellite imageries from 0700TST (UTC+8) to 0810TST (UTC+8) on 2 January 2020 in ten minutes interval over Taiwan area delineated that the upper cloud moved from west to east while the lower cloud shifted from north to south off the east coast of Taiwan Island. The Himawari visible satellite imageries during the same time period told that low and thick cloud layer kept stay over the complex terrains around Hongludi ridge (烘爐地山脊) in altitude of 1166 m (3826 ft) ASL (above sea level). Based upon the mesonet surface data analysis, we learned that the local convergence of prevailing easterly wind and land breeze over the northeast corner of Taiwan was the primary weather circumstance in the early morning, bringing abundant moisture inland, triggering the cloud/fog generation and maintaining its development.

Also, the vertical cross section of relative humidity (%), omega (- μbar/s) and wind speed (kts) along 24.5^{o}N between 120.1^{o}E and 122.5^{o}E based on the WINS (Weather Integration and Nowcasting System) data of Central Weather Bureau at 0200TST (UTC+8) and 0800TST (UTC+8) on 2 January 2020 delivered more reliable evidences, mentioning a locally vertical circulation with obvious upward motions in magnitude of 10^{-2} m/s under the 850 hPa level over the plain area and slight downward motions over the complex terrains. Visibility forecast conducted by NCDR (National Center for Disaster Reduction) offered the visibility difference initiated by the surface fog, and illuminated the worst visibility was in the range of the 0-50 m over the complex terrains.

It preliminarily concludes that the persistent low cloud/fog and the unstable flow over the complex terrain might reduce the reliability of visibility and increased the flight risk in VFR (visual flight rules). Those weather conditions will threat the aviation safety greatly. It implies that during this VIP transport mission the pilots should get ready to conduct IFR (instrument flight rules) mode at any time over the complex terrains. On 15 February 2020, ROC Air Force held a press conference and reported the preliminary investigation, pointing out that the combination of environmental (weather and terrain) and human factors was behind the fatal helicopter accident. The conclusions in the study can confirm the similar scenario on the weather part.

Acknowledgements

We are very grateful to the Central Weather Bureau, the National Science and Technology Center for Disaster Reduction, and the Air Force Weather Wing of ROC for preparing the useful weather maps and satellite imageries. Also, we appreciate that NOAA/ESRL offers the atmospheric variables plotting approach in use of NCEP/NCAR reanalysis data. In addition, some experts and scholars in meteorology and aviation safety gave constructive suggestions to improve this manuscript.

References

Central Weather Bureau, 2020. Online available from: https://www.cwb.gov.tw

Hayes, P., 2019: Helicopter safety and losses: Annual Review 2018. Flight Global. Online available from:https://fg-reports-live.s3-eu-west-1.amazonaws.com/pdf/Helicopter%20Safety%20and%20Losses%202018.pdf

Helicopter Safety News, 2020: Slight change in total U.S. helicopter accidents during 2019. February 2020. The U.S. Helicopter Safety Team. Online available from: http://jayc5.sg-host.com/Press_Releases/2019_Full_Year%20_AccidentRate.pdf

Helicopter Safety News, 2020: A reduction in helicopter operations leads to a reduction in accidents. 13 July 2020. The U.S. Helicopter Safety Team. Online available from: http://jayc5.sg-host.com/Press_Releases/Release6Months2020.pdf

Hogan, P., 2014: Helicopter crashes. Hogan Injury. Online available from: https://www.hoganinjury.com/helicopter-crashes/

Hor, T. H., C. H. Wei, Y. S. Chen, T. Y. Shyu, 2020: Mesoscale analysis on the asymmetric rainband of typhoon Matmo (2014) and the related weather situations for the GE222 aircraft crash case. Universal Journal of Geoscience, 8, 2, 33-44. DOI: 10.13189/ujg.2020.080202

Hsiang, Y., Yu, M., and Lin, K., 2020: Black Hawk crash likely due to human factor, weather: report. Focus Taiwan. Online available from: https://focustaiwan.tw/politics/202002150004

Japan Meteorological Agency, 2016: Basics of Satellite Image Analysis. 29 June 2016. Online available from: www.scribd.com/.../Basics-of-Satellite-Image-Analysis

Lin, C. Y. , C. K. Yu, 2016: Effect of sea surface temperature on the convective lines off the southeastern coast of Taiwan. Atmospheric Sciences, 44, 3, 215-235.

Liu, C. M., 2008: Severe weather and helicopter flight safety - Case study on the ROC Army helicopter accident on 3 April 2007. Aviation Weather, 10, 3-7.

NCDR WATCH, 2020. Online available from: https://watch.ncdr.nat.gov.tw/

NOAA/ESRL. Atmospheric variables plotting page. Online available from: www.esrl.noaa.gov/psd/data/histdata

Tsai, J. H., 2013: The study of the aviation safety in Taiwan government helicopter. Master thesis, Department of Aeronautics and Astronautics, National Chung Kung University. pp.105.

Yu, C. K., and C. Y. Lin, 2008: Statistical location and timing of the convective lines off the mountainous coast of southeastern Taiwan from long-term radar observations. Mon. Wea. Rev., 136, 5077-5094.

Table 1. Annual fatal accident rates (fatal accidents per 100 helicopters at risk) of western-built civil turbine helicopters globally from 2009 to 2018 globally. Here, “single” stands for single-engine helicopters, and “multi” represents multi-engine helicopters. (Referred to Hayes, 2019)

Year	2009	2010	2011	2012	2013	2014	2015	2016	2017	2018
All	0.25	0.29	0.35	0.24	0.28	0.18	0.27	0.23	0.21	0.22
Single	0.27	0.32	0.37	0.29	0.33	0.21	0.33	0.27	0.25	0.24
Multi	0.21	0.23	0.30	0.15	0.19	0.11	0.18	0.17	0.14	0.20

Table 2. Annual accidents, fatal accidents, and fatalities for the US civil helicopter industry from 2013 to 2019. (Referred to the U.S. Helicopter Safety Team, 2020)

Year	2013	2014	2015	2016	2017	2018	2019
Accidents	146	138	121	108	123	121	122
Fatal Accidents	30	21	17	17	20	24	24
Fatalities	62	37	28	29	34	55	51

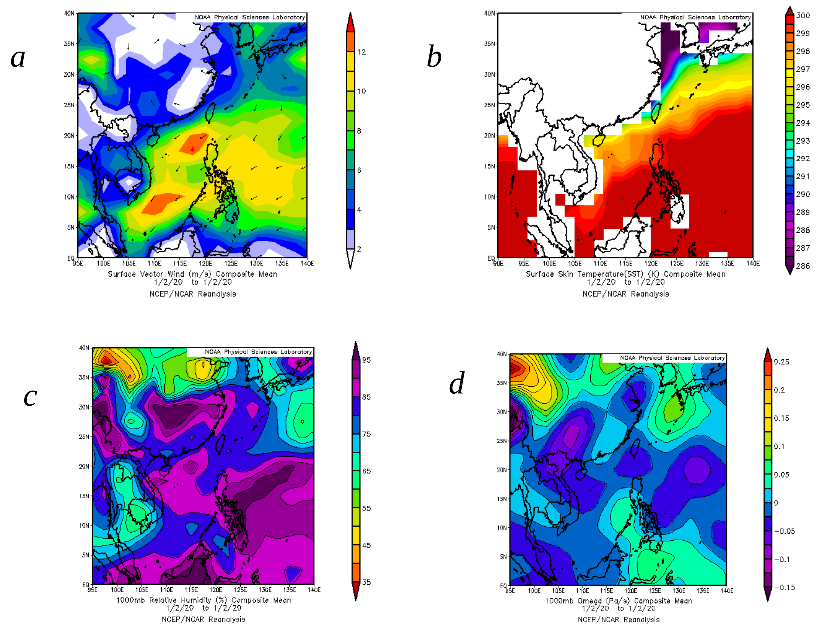

Fig. 1 Composite mean surface vector winds (m/s), sea surface temperature (^{o}C), 1000 hPa-level relative humidity (%), and omega (Pa/s) between EQ-40^{o}N and 95^{o}E-140^{o}E on 02 January 2020. (Resulted from NOAA/ESRL)

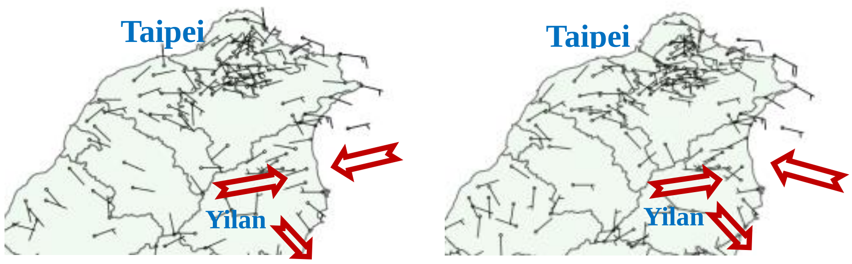

Fig. 2(a) The surface wind map at 0700TST (UTC+8) on 2 January 2020. An obvious convergence zone was formed over the Yilan Plain and the complex terrains. (b) The same as (a) except at 0800TST (UTC+8) on 2 January 2020. (Referred from the NCDR WATCH)

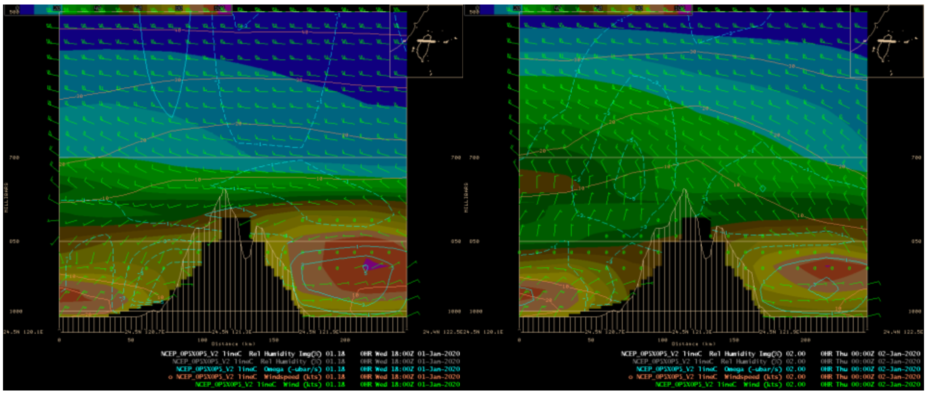

Fig. 3(a) The vertical cross section of relative humidity (%), omega (- ubar/s) and wind speed (kts) along 24.5°N between 120.1°E and 122.5°E based on the WINS (Weather Integration and Nowcasting System) data of Central Weather Bureau at 0200TST (UTC+8) on 2 January 2020. (b) The same as (a) except at 0800TST (UTC+8) on 2 January 2020. (Resulted from CWB/WINS)

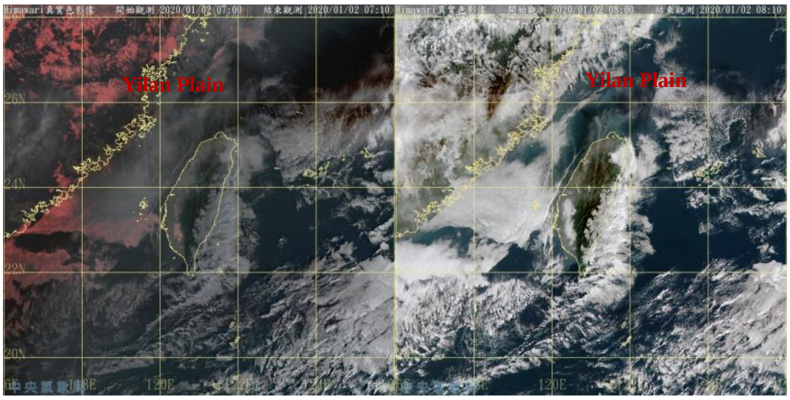

Fig. 4(a) Himawari true color satellite image at 0700TST (UTC+8) on 2 January 2020. (b) The same as (a) except at 0800TST on 2 January 2020. (Referred from the Central Weather Bureau)